Available online at www.sciencedirect.com

SciVerse ScienceDirect

Nuclear Physics A 895 (2012) 20–32

NUCLEAR PHYSICS A

www.elsevier.com/locate/nuclphysa

The relationship between the interacting boson model and the algebraic version of Bohr's collective model in its triaxial limit

G. Thiamova [a,*], D.J. Rowe [b], M.A. Caprio [c]

[a] *LPSC, Université Joseph Fourier Grenoble 1, CNRS/IN2P3, Institut National Polytechnique de Grenoble, F-38026 Grenoble Cedex, France*

[b] *Department of Physics, University of Toronto, Toronto, ON M5S 1A7, Canada*

[c] *Department of Physics, University of Notre Dame, Notre Dame, IN 46556-5670, USA*

Received 7 August 2012; received in revised form 10 September 2012; accepted 10 September 2012

Available online 14 September 2012

Abstract

Recent developments and applications of an algebraic version of Bohr's collective model, known as the algebraic collective model (ACM), have shown that fully converged calculations can be performed for a large range of Hamiltonians. Examining the algebraic structure underlying the Bohr model (BM) has also clarified its relationship with the interacting boson model (IBM), with which it has related solvable limits and corresponding dynamical symmetries. In particular, the algebraic structure of the IBM is obtained as a compactification of the BM and conversely the BM is regained in various contraction limits of the IBM. In a previous paper, corresponding contractions were identified and confirmed numerically for axially-symmetric states of relatively small deformation. In this paper, we extend the comparisons to realistic deformations and compare results of the two models in the rotor–vibrator limit. These models describe rotations and vibrations about an axially symmetric prolate or oblate rotor, and rotations and vibrations of a triaxial rotor. It is determined that most of the standard results of the BM can be obtained as contraction limits of the IBM in its $U(5)$–$SO(6)$ dynamical symmetries.

Keywords: Interacting boson model; Bohr collective model; Algebraic collective model; Triaxial nuclear deformation

* Corresponding author.
E-mail address: gabriela.thiamova@grenoble-inp.fr (G. Thiamova).

0375-9474/$ – see front matter © 2012 Elsevier B.V. All rights reserved.
http://dx.doi.org/10.1016/j.nuclphysa.2012.09.002

1. Introduction

The Bohr collective model (BM) [1] and its unified extensions [2], developed by Bohr and Mottelson and numerous colleagues, provide the essential tools for a phenomenological description of nuclear collective structure [3,4]. The interacting boson model (IBM) [5,6] was also introduced to describe collective properties of nuclei. The key ingredients of the IBM and its many extensions are their algebraic structure and the ease with which calculations can be made using the powerful methods of group theory.

Similarly, the algebraic collective model (ACM), introduced as a computationally tractable version of the BM [7–9] restricted to rotational and quadrupole vibrational degrees of freedom, is characterized by a well-defined algebraic structure (see Ref. [10] for a review of this model). Unlike the conventional $U(5) \supset SO(5) \supset SO(3)$ dynamical subgroup chain used, for example, in the Frankfurt program [11,12], the ACM makes use of the subgroup chain

$$SU(1,1) \times SO(5) \supset U(1) \times SO(3) \supset SO(2) \tag{1}$$

to define basis wave functions as products of β wave functions and $SO(5)$ spherical harmonics. Several advantages result from this choice of dynamical subgroup chain: (i) with the now available $SO(5)$ Clebsch–Gordan Coefficients [13,14], and explicit expressions for β matrix elements and $SO(5)$ reduced matrix elements, matrix elements of BM operators can be calculated analytically; (ii) by appropriate choices of $SU(1,1)$ modified oscillator representations, the β basis wave functions range from those of the $U(5) \supset SO(5)$ harmonic vibrational model to those of the rigid-β wave function of the $SO(5)$-invariant Wilets–Jean model; and (iii) with these $SU(1,1)$ representations, collective model calculations converge an order of magnitude more rapidly for deformed nuclei than in $U(5) \supset SO(5)$ bases. Thus, the ACM combines the advantages of the BM and the IBM and makes collective model calculations a simple routine procedure [7,8,15,16].

Close parallels between the IBM-1 version of the IBM and the BM were recognized already at the time the IBM was conceived [17–19] and subsequently explored by many authors (see, for example, Refs. [20–22]). In particular, the $SO(6)$ limit of the IBM was observed [23] to be closely related to the β-rigid Wilets–Jean model [24]. In Ref. [25] the states of the IBM-1 in its various dynamical symmetry limits were identified with subsets of BM states of corresponding dynamical symmetries. The aim was to identify maps which give the contractions of the IBM in the limit of large boson number and for which corresponding observables are simultaneously simple in both models. Such an identification is important because the IBM can be viewed as a truncated equivalent of the BM. However, in principle there are infinitely many ways to map the IBM into the BM. Such maps are significant, especially if the two models give alternative physical interpretations of nuclear data.

For a reliable comparison of the ACM and the IBM contraction limits, it is essential to be able to perform calculations for high boson numbers. In a recent paper [26] we considered such a comparison for axially symmetric representations. We consider here their extension to triaxial nuclei. For this purpose, we make use of the $SO(5)$ Clebsch–Gordan (CG) coefficients that are readily available up to $v_{\max} = 200$ [13,14]. Thus, collective model calculations can be carried out easily and quickly both in the IBM and the ACM [7,16] using the known analytical expressions for $SO(5)$ reduced matrix elements [9,16,25,27].

In the ACM, fully converged calculations were performed in Ref. [16] for a range of Hamiltonians to determine the extent to which experimental data can be realistically described in terms of the BM. More importantly, they prepare the way for more general, but still solvable, algebraic collective models that include intrinsic degrees of freedom as in the unified model of Bohr and Mottelson [3,4].

In this paper we perform calculations in the $SO(6)$ limit of the IBM, following Ref. [28], to describe rotations and vibrations of a triaxially deformed nucleus. We compare the results with parallel calculations carried out within the ACM and show that, for modest interaction strengths and large enough boson number, the IBM calculations converge to those of the ACM.

2. Methods

The IBM calculations for large boson numbers are carried out with Hamiltonians obtained directly from corresponding ACM Hamiltonians. The IBM in its $SO(6)$ limit has a well-defined embedding in the BM [25]. However, a direct mapping of a single $SO(6)$ irreducible representation (irrep) into an irrep of the β-rigid Wilets–Jean model does not give the appropriate map, first because an IBM $U(6)$ irrep contains many $SO(6)$ irreps and second, because β-rigid wave functions are delta functions that do not have convergent expansions on any orthonormal basis of the BM. The ACM provides a way to circumvent this problem. The solution is to replace the conventional $U(6) \supset SO(6) \supset SO(5) \supset SO(3)$ dynamical group chain by the dual chain (1). This replacement makes use of a known duality between irreps of $SU(1,1)$ and $SO(6)$ and between irreps of $U(1)$ and $U(6)$ on the space of the six-dimensional harmonic oscillator. This duality implies that the above mentioned pairs of irreps share the same quantum number; $SU(1,1)$ and $SO(6)$ irreps can be simultaneously labeled by a common seniority quantum number σ and $U(1)$ and $U(6)$ share the same quantum number N corresponding to the IBM boson number. The required mapping into the BM now becomes clear because the irreps of the dual chain (1) can be mapped to the corresponding irreps of an isomorphic dynamical chain used in the ACM to define a continuous sequence of bases for the BM.

The treatment given in Ref. [26] was limited to axially symmetric rotors. Nevertheless, in the extension to triaxial rotors presented here, the $SO(5)$ kinetic energy is again the $SO(5)$ Casimir invariant, $\hat{\Lambda}$, and the potential energy is the same $SO(3)$-invariant function of the quadrupole operators as used in the ACM. This correspondence is consistent with the suggestion of Van Isacker [29] (see also [30–32]) to include a cubic $(\hat{Q} \otimes \hat{Q} \otimes \hat{Q})_0 \propto \cos 3\gamma$ term in the IBM $SO(6)$ Hamiltonian, with the quadrupole operators defined in the standard way as elements of the $SO(6)$ algebra by $\hat{Q}_\mu = d^\dagger_\mu \tilde{s} + s^\dagger \tilde{d}_\mu$.

Such Hamiltonians with both linear and quadratic terms in $(\hat{Q} \otimes \hat{Q} \otimes \hat{Q})_0$ have been used in the ACM [16] and in corresponding IBM Hamiltonians [28]. It is shown here and in Refs. [28, 25], that with increasing boson number the IBM results approach those of the ACM. It has also been shown [16] that with a high degree of rigidity in the β degree of freedom and large linear or quadratic terms in $(\hat{Q} \otimes \hat{Q} \otimes \hat{Q})_0$, but not both, the results of the ACM approach those of symmetric tops. With a large linear term in $(\hat{Q} \otimes \hat{Q} \otimes \hat{Q})_0$ they approach those of an axially symmetric rigid rotor and with a large quadratic term they approach those of a triaxial Meyer-ter-Vehn ($\gamma = 30^\circ$) rotor [33]. More generally, the results of both models approach those of triaxial Davydov–Filippov rigid rotor models [34,35].

2.1. A brief description of the models

2.1.1. ACM calculations

In the BM it is customary to introduce intrinsic quadrupole coordinates β and γ that are directly related to the deformation parameters and to quadrupole moments [36]. It follows that a potential in β and γ is a function of the rotational invariants β^2 and $\cos 3\gamma$ defined in terms of the quadrupole tensor operator $\hat{Q}$ by

$$\hat{Q}\cdot\hat{Q}=\beta^2, \qquad (\hat{Q}\otimes\hat{Q}\otimes\hat{Q})_0=-\sqrt{\frac{2}{35}}\beta^3\cos 3\gamma. \tag{2}$$

A β-dependent ACM Hamiltonian is given, for example, in the form

$$\hat{H}(B,\alpha,\kappa,\chi)=\frac{-\nabla^2}{2B}+\frac{1}{2}B\big[(1-2\alpha)\beta^2+\alpha\beta^4\big]-\kappa\beta\cos 3\gamma+\chi\cos^2 3\gamma, \tag{3}$$

where

$$\nabla^2=\frac{1}{\beta^4}\frac{\partial}{\partial\beta}\beta^4\frac{\partial}{\partial\beta}+\frac{1}{\beta^2}\hat{\Lambda} \tag{4}$$

is the Laplacian on the five-dimensional collective model space [10] and the operator $\hat{\Lambda}$ represents the Casimir operator of the five-dimensional rotation group $SO(5)$ whose $SO(3)$ subgroup contains the rotations in physical space described by Euler angles. Such a Hamiltonian, expressed in terms of the quadrupole deformation parameters β and γ serves as a useful starting point for a description of a wide range of nuclear collective spectra.

A Hamiltonian of this form was used [37], for example, to study the second-order phase transition of a model nucleus, from a spherical to a deformed phase, with α as a control parameter. For $\alpha=0$ the potential is that of a spherical harmonic oscillator, $\frac{1}{2}B\beta^2$, while for $\alpha>0.5$ it has a minimum for a non-zero value of β, which increases as α increases. Moreover, as the mass parameter B of the Hamiltonian (5) increases, the kinetic energy decreases and the result is a decrease of the vibrational β fluctuations of the model about its equilibrium deformation. Thus, the value of the parameter α controls the β deformation of the model and the parameter B controls its rigidity. Thus, by adjusting the parameters α and B a model with any equilibrium value of the β deformation and any degree of rigidity may be constructed. In Ref. [16] it has been shown that parameter values in the range $0<\alpha<2.0$ and $10<B<100$ are sufficient to describe the β deformations and rigidities of observed nuclear collective states.

2.1.2. ACM calculations in the β-rigid limit

In making comparisons with the $SO(6)$ limit of the IBM, it is appropriate to reduce the β-dependent ACM Hamiltonian (3) to angular variables. In this way, the β-rigid limit of the Hamiltonian (3) is effectively obtained. If β is assigned a fixed value, which may be taken to be $\beta=1$, then the rotational invariants (2) built from the quadrupole operator reduce to $\hat{Q}\cdot\hat{Q}=1$ and $(\hat{Q}\otimes\hat{Q}\otimes\hat{Q})_0=-\sqrt{\frac{2}{35}}\cos 3\gamma$. Thus, a Hamiltonian in angular variables built from rotational invariants has the form $\hat{H}=\hat{\Lambda}+a_1(\hat{Q}\otimes\hat{Q}\otimes\hat{Q})_0+a_2[(\hat{Q}\otimes\hat{Q}\otimes\hat{Q})_0]^2+\cdots$, and a β-dependent Hamiltonian such as (3) reduces to this form. We take the specific parametrization [38]

$$\hat{H}_{\mathrm{ACM}}=\hat{\Lambda}+\chi\big[(1-\cos 3\gamma)+\xi\cos^2 3\gamma\big] \tag{5}$$

which includes an additive constant for convenience (in providing a positive-definite potential). The above Hamiltonian has been used in Ref. [38] to obtain quantitative predictions for phonon and multiphonon excitations in well-deformed rotor nuclei and to investigate the coupling of the dynamical γ deformation and the rotational motion. Such an approximation may be considered for well-deformed nuclei. It has also been proposed [39] for use in studying the axial–triaxial shape transition, along the lines of the work here.

2.1.3. The IBM description of axially-symmetric and triaxial nuclei in the $SO(6)$ limit

It has been shown in Ref. [25] that in the IBM → BM contraction of the $SO(6)$ Lie algebra, the BM image of the $SO(6)$ cubic term $(\hat{Q}\otimes\hat{Q}\otimes\hat{Q})_0$ is given by

$$(\hat{Q}\otimes\hat{Q}\otimes\hat{Q})_0 \to -\sqrt{\frac{2}{35}}\big[\sigma(\sigma+4)\big]^{3/2}\cos 3\gamma. \tag{6}$$

This implies that the $SO(6)$ limit corresponds to the β-rigid limit of the ACM in which $\beta \to [\sigma(\sigma+4)]^{1/2}$.

Thus, we consider an $SO(6)$-conserving IBM Hamiltonian

$$\hat{H}_{\mathrm{IBM}} = \hat{\Lambda} + \kappa(\hat{Q}\otimes\hat{Q}\otimes\hat{Q})_0 + \xi'\big[(\hat{Q}\otimes\hat{Q}\otimes\hat{Q})_0\big]^2, \tag{7}$$

where $\hat{\Lambda}$ now represents the $SO(5)$ Casimir operator of the IBM and $\hat{Q}$ now represents the IBM quadrupole operator $\hat{Q}_\mu = d^\dagger_\mu\tilde{s} + s^\dagger\tilde{d}_\mu$, and we will compare the results obtained, for increasing N, with those of ACM calculations for the Hamiltonian $\hat{H}_{ACM}$ (5) above. Within a given $SO(6)$ irreducible representation σ the identification between κ and ξ' coefficients of (7) and the χ and ξ coefficients of (5) is then

$$\kappa = \frac{\chi}{F}, \qquad \xi' = \frac{\chi\xi}{F^2}, \tag{8}$$

where

$$F = -\sqrt{\frac{2}{35}}\big[\sigma(\sigma+4)\big]^{3/2}. \tag{9}$$

These identifications will be assumed throughout the remainder of this article, when comparing IBM and ACM calculations.

Note that the IBM spectra are repeated for $SO(6)$ representations $\sigma = N, N-2, N-4, \ldots,$ where N is the total boson number, but only the $\sigma = N$ spectra will be shown. If either κ or ξ' are non-zero, the $SO(5)$ seniority quantum numbers v (often denoted by τ in the IBM literature) are mixed. Since $v = \sigma, \sigma-1, \sigma-2, \ldots, 0$ within an $SO(6)$ irrep, the highest value of an admixed seniority $v_{\max}$ occurs in the irrep $\sigma = N$ and is given by $v_{\max} = N$.

3. Results

In this section the results obtained with the IBM Hamiltonian (7) are compared to their ACM counterparts of Hamiltonian (5). It is expected that the IBM results will approach those of the β-rigid ACM in the $N \to \infty$ limit in which the IBM cubic term is related to its ACM $\cos 3\gamma$ image by the relation (6).

The possible shapes of the potential appearing in the Hamiltonian (5) are shown in Fig. 1. For $\xi = 0$ the potential has a minimum at $\gamma = 0°$, i.e. it corresponds to an axially symmetric shape [Fig. 1(a)]. It is also seen that with increasing χ the potential becomes deeper and provides more confinement of the wave function about the minimum. Similar conclusions hold for a triaxial potential. A potential which is simply proportional to $\cos^2 3\gamma$ has a minimum at $\gamma = 30°$ [Fig. 1(b)]. In the general case of (5), in which both χ and ξ are non-zero [Fig. 1(c)], the minimum remains at $\gamma = 0°$ for $\xi \leqslant 0.5$ but moves to non-zero γ as ξ increases past 0.5, approaching 30° as $\xi \to \infty$. For a fixed value of the parameter ξ, the potential becomes deeper with increasing χ. For each of the potentials in Fig. 1, the energetically-accessible range of γ values obtained for the ground state is indicated by the dotted line, which is drawn at the energy obtained for the

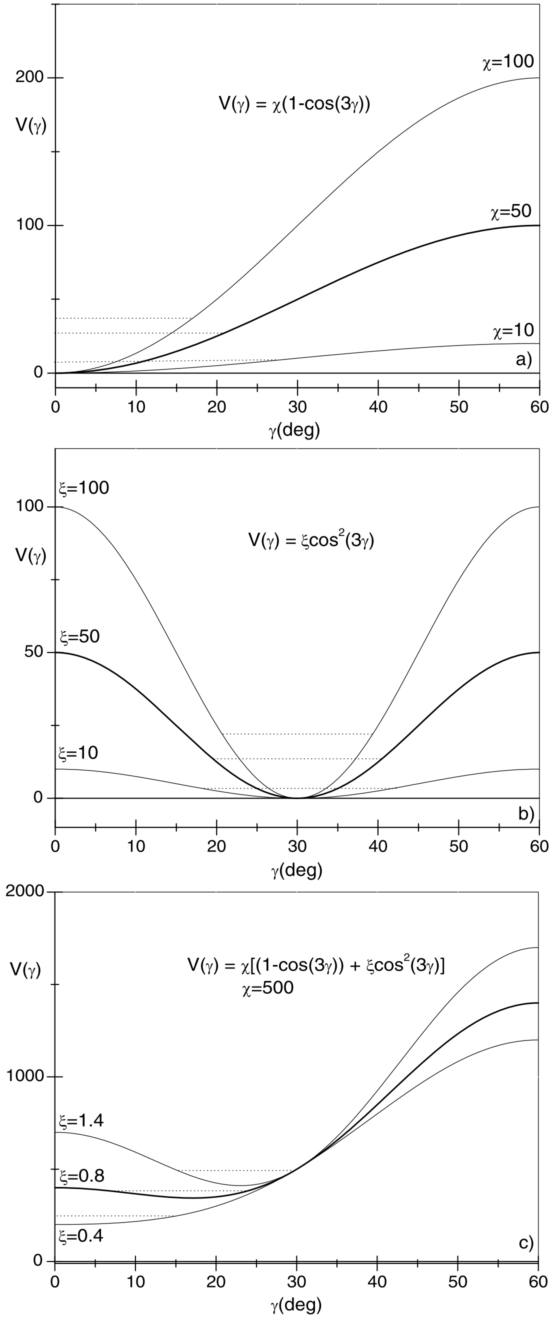

Fig. 1. Potentials $V(\gamma)$ for the ACM Hamiltonian: (a) potentials $V(\gamma) = \chi(1 - \cos 3\gamma)$ with minimum at $\gamma = 0°$, of varying depth, shown for $\chi = 10$, 50, and 100, corresponding to $\xi = 0$ in (5). (b) Potentials $V(\gamma) = \xi \cos^2 3\gamma$ with minimum at $\gamma = 30°$, of varying depth, shown for $\xi = 10$, 50, and 100. (c) Potentials involving both $\cos 3\gamma$ and $\cos^2 3\gamma$ contributions, of varying ratios determined by ξ in (5), shown for $\xi = 0.4$, 0.8, and 1.4, all with $\chi = 500$. The energy eigenvalues obtained for the ground state, with unit coefficient on the kinetic term as in (5), are indicated by the dotted lines, which display the energetically-accessible ranges of γ values for the ground state.

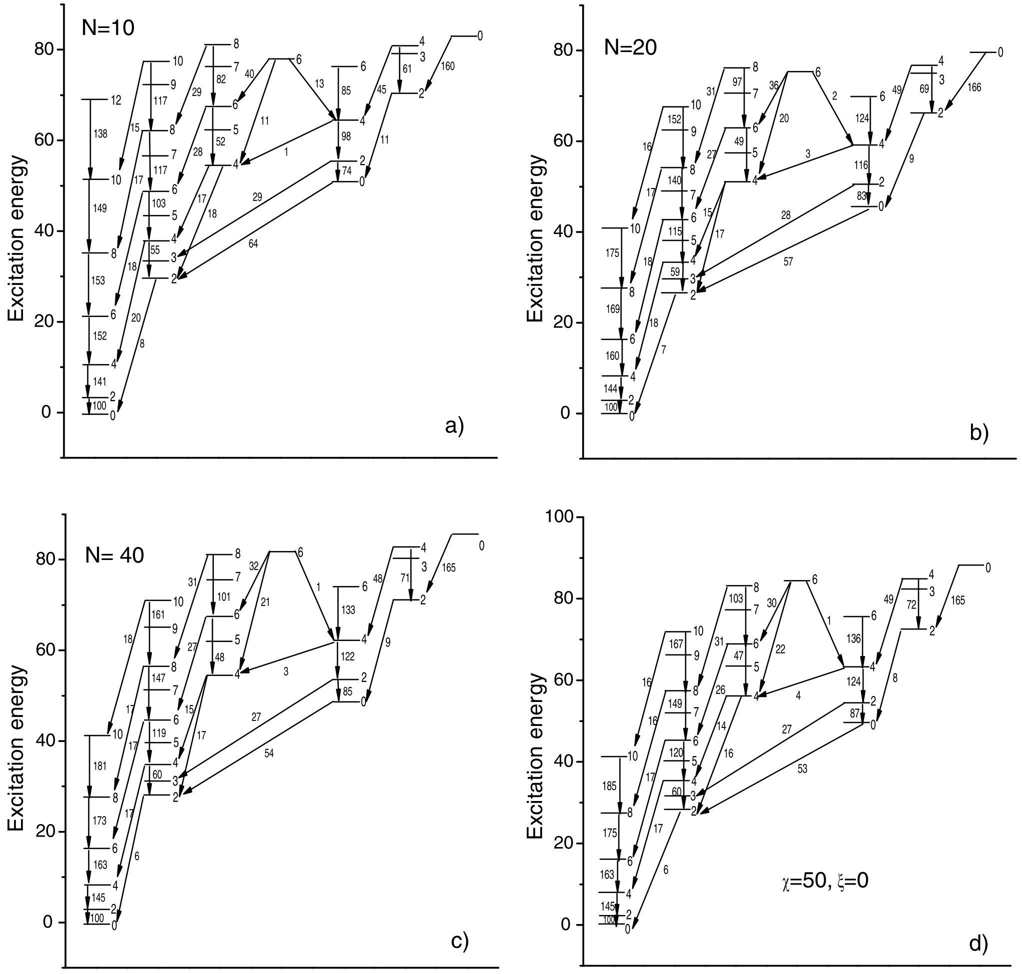

Fig. 2. Excitation energies and $E2$ strengths obtained for an axial rotor–vibrator: for the IBM with $N = 10$ (a), $N = 20$ (b), and $N = 40$ (c), and in the ACM with $\chi = 50$ and $\xi = 0$ (d), as in Fig. 1(a). The parameters for the IBM calculation, at each value of N, are chosen according to the contraction mapping as defined in Section 2.1.3.

ground state. It is seen that the potentials in Fig. 1 are thus quite γ soft, implying substantial interaction between the vibrational and rotational degrees of freedom [38].

When $\gamma = 0^\circ$ or 60° the models exhibit rotations and coupled γ vibrations about an axially symmetric shape. In considering the approach to this limit in the ACM, we consider the ACM Hamiltonian (5) with $\chi = 50$ and $\xi = 0$. The ACM spectrum obtained with this set of parameters is shown in Fig. 2(d). It is compared with its IBM counterparts for $SO(6)$ irreps with $N = 10$, $N = 20$ and $N = 40$ in Fig. 2(a)–(c).

An overall agreement between both sets of calculations is good already for $N = 10$. However, an inspection reveals important deviations from the ACM results. The IBM excitation energies are typically about 20–30% above their ACM analogues. The intraband transition rates between low-energy levels are off by less then 10% while the interband transition rates differ by more than 20%.

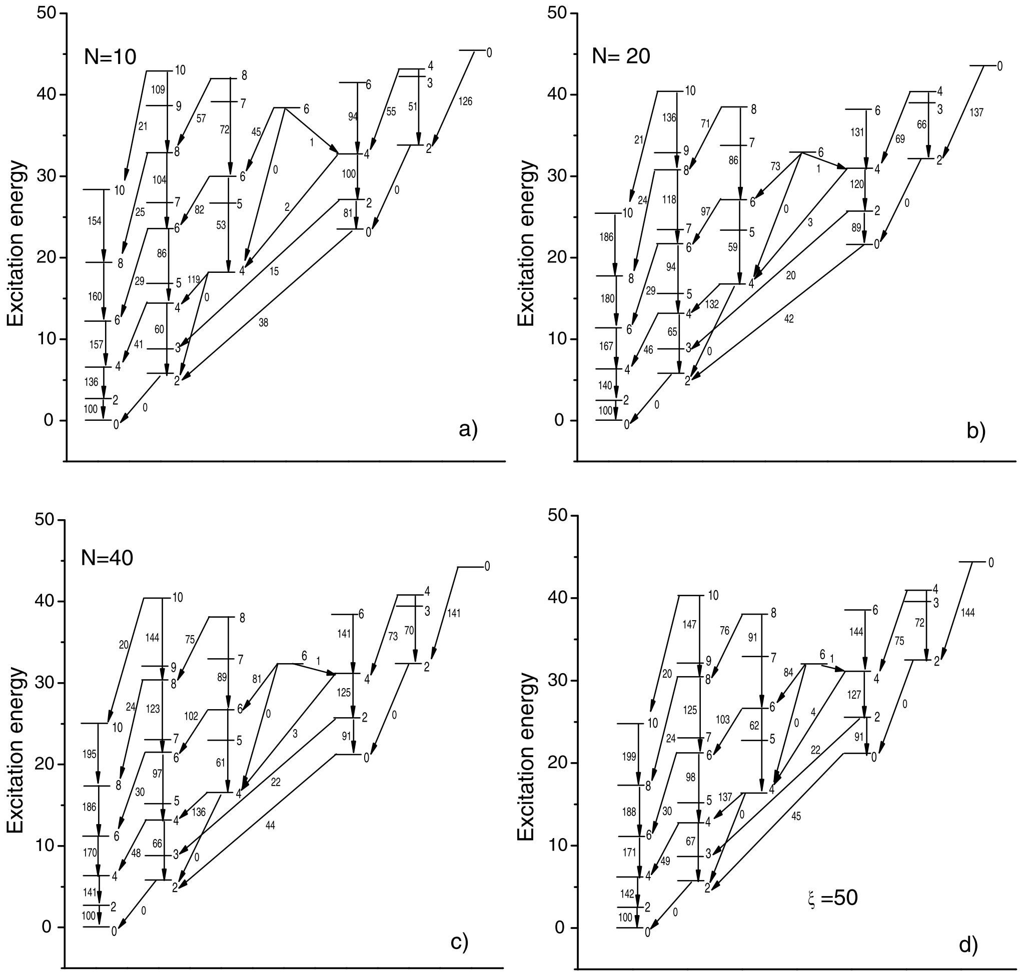

Fig. 3. Excitation energies and $E2$ strengths obtained for a triaxial rotor–vibrator with equilibrium $\gamma = 30°$: for the IBM with $N = 10$ (a), $N = 20$ (b), and $N = 40$ (c), and in the ACM with potential $V(\gamma) = \xi \cos^2 3\gamma$, for $\xi = 50$ (d), as in Fig. 1(b). The parameters for the IBM calculation, at each value of N, are chosen according to the contraction mapping as defined in Section 2.1.3.

A substantial improvement of the agreement between the axially symmetric IBM and the ACM spectra is observed for $N = 20$, and for $N = 40$ both types of spectra are basically identical up to the highest spins shown ($J \sim 10$). In particular, the intraband transition rates of the IBM increase with J at about the same rate as those of the ACM, being smaller by only 2–3% for the highest states. This is a signature that the IBM results have essentially converged to their β-rigid BM counterparts for $N > 20$.

A rotor is said to be a symmetric top if two of its moments of inertia are equal. Symmetric tops have special properties because if two moments of inertia are equal then the component K of the angular momentum along the symmetry axis of the inertia tensor is a good quantum number. We now consider the solution of the BM with mean equilibrium deformation parameter $\gamma = 30°$, for the potential $V(\gamma) = \xi \cos^2 3\gamma$ with $\xi = 50$ of Fig. 1(b). [Note that the parametrization (5) only gives a pure $\cos^2 3\gamma$ potential as a limiting case ($\chi \to 0$ with $\xi \to \infty$), so the meaning of the parameter ξ has been redefined for this example.] This solution is that of a symmetric top even though its quadrupole moments are not those of an axially symmetric rotor [33]. Its ACM spectrum is shown in Fig. 3(d). The figure is plotted such that each energy level of angular momentum L in its first column is the band-head for a rotational band of levels with $K = L$. For example, the $L = 0$ ground state is the band-head for the $K = 0$ sequence of states of $L = 0, 2, 4, 6, \ldots,$ which in the figure are linked by arrows indicating zero $E2$ transitions rates between them. (This is discussed below.) Similarly, the first excited $L = 2$ state is the band-head for a $K = 2$ sequence of states of $L = 2, 3, 4, 5, 6, \ldots,$ which also have zero $E2$ transitions rates between them (not shown in the figure). The corresponding IBM results are shown in Fig. 3(a)–(c).

A common characteristic of the ACM (see Ref. [16]) and the IBM results in this limit is the absence of $E2$ transitions between states of a common K band and the vanishing of all quadrupole moments, as is the case for the rigid Meyer-ter-Vehn rotor [33]. As pointed out in Ref. [16], this is a consequence of an R^5 parity selection rule. The R^5 parity operator is the element of the $O(5) \supset SO(5)$ group that transforms vectors in R^5 to their negatives. Thus, in the absence of the term $(\hat{Q} \otimes \hat{Q} \otimes \hat{Q})_0$ in the Hamiltonian, the Hamiltonian is invariant under R^5 inversion and its eigenstates all have good R^5 parity. In parallel with the $O(3)$ inversion operator on R^3, for which states of $SO(3)$ angular momentum l have parity $(-1)^l$, the states of $SO(5)$ seniority v have R^5 parity $(-1)^v$. As remarked in [16] and derived in [10] the states of this triaxial symmetric top have R^5 parity $(-1)^{K/2+n_\gamma}$, where n_γ is the γ phonon number. (There are no β-vibrational excitations in this rigid-β model.) Thus, because the quadrupole operator is of negative R^5 parity, it has vanishing matrix elements between all states of the same R^5 parity and vanishing expectation values in all states. A parallel result is obtained in the IBM with respect to its $O(5)$ parity which is likewise given for states of $SO(5)$ seniority v by $(-1)^v$. In the IBM this R^5 parity is often referred to as d parity.

For the allowed $E2$ transitions in Fig. 3, the degree of agreement between the ACM and the IBM calculations for $N = 10$, $N = 20$ and $N = 40$ is quantitatively similar to that expressed for the axially symmetric case. For $N = 10$ IBM calculations important departures from the ACM excitation energies and transition rates are present but both models provide essentially identical results up to highest spins shown for $N = 40$.

A generic triaxial situation in which both χ and ξ are non-zero is shown in Fig. 4. The ACM calculations have been made with a set of parameters $\chi = 500$ and $\xi = 0.8$ [Fig. 4(d)]. The corresponding IBM calculations are shown in Fig. 4(a)–(c). Similarly to the two previous cases the $N = 40$ IBM spectrum is well contracted to its ACM counterpart.

The level energies and transition observables provide only indirect measures of the evolving structure of the nuclear eigenstates. It is informative to consider also a more direct measure of the deformation — in particular the triaxiality — obtained in the IBM calculations, to observe how the intrinsic structure approaches the ACM limit. The expectation values of the quadrupole shape invariants $\hat{Q} \cdot \hat{Q}$ and $(\hat{Q} \otimes \hat{Q} \otimes \hat{Q})_0$ from (2) as well as higher-order scalar products of Q, have commonly been used [40,41] to extract information on mean values and variances for the β and γ variables, including in prior studies with the IBM [42–44] and ACM [38]. Here, of course, only the γ degree of freedom is relevant. We consider the lowest-order invariant $\cos 3\overline{\gamma} = -\sqrt{\frac{35}{2}}\langle(\hat{Q} \otimes \hat{Q} \otimes \hat{Q})_0\rangle$ which defines an effective or "mean" γ value $\overline{\gamma}$. The evolution of the results of the IBM calculations towards the ACM values, with increasing N, is shown in Fig. 5 for the axially symmetric case of Fig. 2(d) and the triaxial case of Fig. 4(d). By $N = 40$, the triaxiality of the IBM calculations is consistently approaching that of the ACM calculations, as

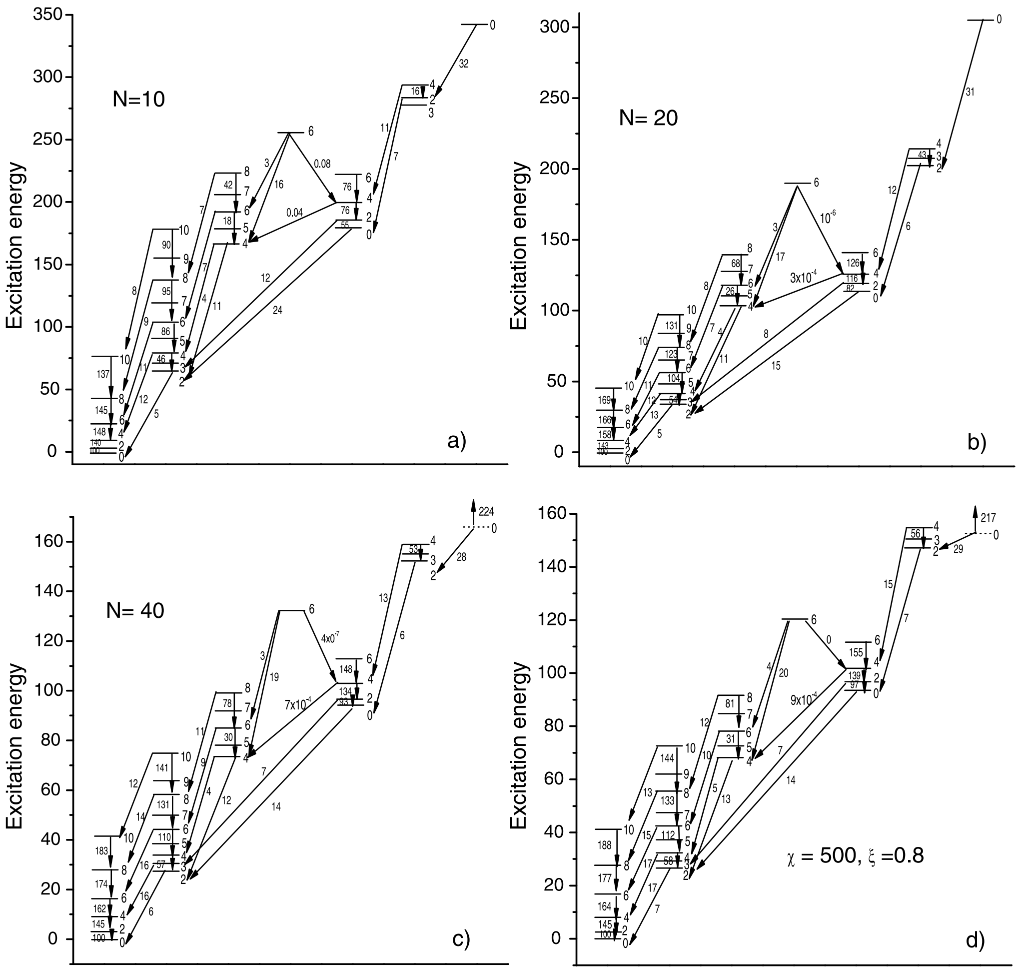

Fig. 4. Excitation energies and $E2$ strengths obtained for a generic triaxial rotor–vibrator: for the IBM with $N = 10$ (a), $N = 20$ (b), and $N = 40$ (c), and in the ACM with $\chi = 500$ and $\xi = 0.8$ (d), as in Fig. 1(c). The parameters for the IBM calculation, at each value of N, are chosen according to the contraction mapping as defined in Section 2.1.3.

seen for the ground state and $K = 0$ two γ-phonon band-head states in Fig. 5. Quite large values of $\bar{\gamma}$ are obtained [38,44] that are consistent with the large range of energetically accessible values of γ in the case of the γ-soft calculations we present here.

4. Discussion

In this paper we have performed calculations in the $SO(6)$ limit of the IBM, to describe rotations and vibrations of an axially symmetric and triaxially deformed nucleus. Those calculations have been compared to the results obtained within the ACM to show that, for modest interaction strengths and large enough boson number ($N \approx 40$), the IBM calculations converge to those of the ACM. The level energies and transition observables obtained within the IBM for $N = 10, 20$ and 40 have been presented to demonstrate the evolution of the structure of the nuclear eigen-

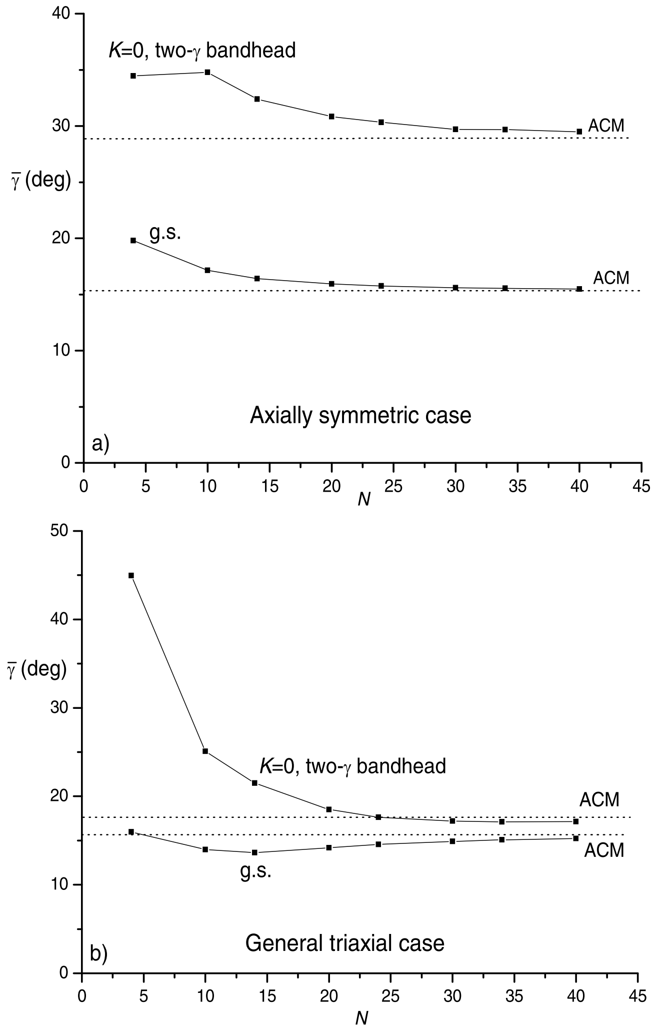

Fig. 5. Effective γ values obtained in IBM calculations with increasing boson number (solid curves), over the range $4 \leqslant N \leqslant 40$, illustrating their approach to the value obtained in the ACM contraction limit (dotted lines): (a) for the axial rotor–vibrator with $\chi = 50$ and $\xi = 0$, considered in Fig. 2, and (b) for the generic triaxial rotor–vibrator with $\chi = 500$ and $\xi = 0.8$, considered in Fig. 4.

states towards their ACM counterparts. As a more direct measure of the closeness of the IBM and the ACM results, the progression of the IBM effective γ values to the corresponding ACM value with increasing N has also been shown.

It is of interest to relax the β-rigid constraint in comparing results of the ACM and large-N IBM calculations and also explore the relationship between the BM and the IBM in its $SU(3)$ limit. The former can be done by augmenting the quadrupole operators of the IBM from the $SO(6)$-conserving operators $\{\hat{Q}_m = d_m^\dagger s + s^\dagger d_m\}$, used here, to include the operators $\{(\hat{d}^\dagger \otimes d)_{2m}\}$. Such operators then have non-zero transition matrix elements between states of different $SO(6)$ irreps which correspond to states of different β-vibrational quantum numbers.

Note that in ACM calculations involving the β degree of freedom, with the Hamiltonian (3), a large centrifugal stretching is observed [16] for small values of the mass parameter B, which is suppressed in the β-rigid approximation. The effects of centrifugal stretching are seen, for example, in a comparison of the energy levels of the excited states that fall increasingly below those of the β-rigid approximation as the angular momentum is increased [16]. It is observed that the β and γ excitation energies increase with increasing α and κ and, for large values of these parameters, approach the adiabatic β-rigid limit of the BM. Similar results are expected for IBM calculations for which the adiabatic limit of the BM is approached with increasing boson number and the strength of the parameter κ [25,26,28]. In fact, for small boson numbers, as in Fig. 2(a), a rapid decrease of the intraband IBM transition rates beyond their ACM counterparts is observed between high spin levels.

It is commonly understood that the IBM and BM have much in common and that, for a large value of N, the IBM contracts to the BM. However, our analysis and that of the previous paper [26] have shown that the mappings between the two models for which the two models become algebraically equivalent in the $N \to \infty$ limit are very different for the $U(5)$ and $SO(6)$ dynamical symmetry chains of the IBM. We have also found, but have not shown here, that there is yet another mapping for the $SU(3)$ dynamical limit. These several relationships, and the fact that the IBM rapidly approaches its asymptotic limits for modest values of N, is a strong indication that it would be difficult to assess which of the two models is more successful in fitting any finite amount of data. Our findings indicate that, if N in the IBM is assigned a fixed value ($\gtrsim 10$), the two models are likely to agree with each other more closely than with the body of experimental data. At the same time we recognize that, if N were treated as an adjustable parameter, the IBM would have an extra degree of freedom that could be used to advantage to obtain better detailed fits. It is also important to recall, as mentioned above, that our present comparisons have been between the $SO(6)$ limit of the IBM and the β-rigid limit of the BM. In view of the strong experimental evidence of non-adiabatic coupling between the rotational and β-vibrational degrees of freedom, *e.g.*, due to centrifugal forces, detailed comparisons with data should take account of this coupling.

The significant result of our findings is that two models, with very different physical foundations, can have closely related algebraic structures. This highlights the fact, that to learn from the successes of either model, it is important to go beyond their ability to fit experimental data in a straightforward way. For example, one should consider the physical interpretation of the model variables and their extensions to higher order. The expectation is that the algebraic structures of the models will naturally extend in different ways and lead to distinguishable model predictions. For example, the nucleon-pair interpretation of the IBM bosons has strong implications for two-nucleon transfer cross sections, whereas the interpretation of the Bohr model shape coordinates as quadrupole moments, as in the ACM, has implications for sum rules. Another significant observation is that the IBM has two ways of describing nuclear rotations: one in its $SO(6)$ limit, as we have discussed, and one in its $SU(3)$ limit. This raises the question as to the physical difference between the two limits and when to use one and when the other.

Acknowledgements

This work was supported in part by the US DOE under grant DE-FG02-95ER-40934.

References

[1] A. Bohr, Mat. Fys. Medd. K. Dan. Vidensk. Selsk. 26 (14) (1952).
[2] A. Bohr, B.R. Mottelson, Mat. Fys. Medd. K. Dan. Vidensk. Selsk. 27 (16) (1953).
[3] A. Bohr, B.R. Mottelson, Nuclear Structure: Nuclear Deformations, vol. 2, World Scientific, Singapore, 1998.
[4] D.J. Rowe, Nuclear Collective Motion: Models and Theory, Methuen, London, 1970, reprinted by World Scientific, Singapore, 2010.
[5] F. Iachello, A. Arima, The Interacting Boson Model, Cambridge University Press, 1987.
[6] A. Arima, F. Iachello, Ann. Phys. (N. Y.) 99 (1976) 253;
A. Arima, F. Iachello, Ann. Phys. (N. Y.) 11 (1978) 201;
A. Arima, F. Iachello, Ann. Phys. (N. Y.) 123 (1979) 468.
[7] D.J. Rowe, Nucl. Phys. A 735 (2004) 372.
[8] D.J. Rowe, P.S. Turner, Nucl. Phys. A 753 (2005) 94.
[9] D.J. Rowe, J. Phys. A: Math. Gen. 38 (2005) 10181.
[10] D.J. Rowe, J.L. Wood, Fundamentals of Nuclear Models: Foundational Models, World Scientific, Singapore, 2010.
[11] G. Gneuss, W. Greiner, Nucl. Phys. A 171 (1971) 449.
[12] P.O. Hess, J.A. Maruhn, W. Greiner, J. Phys. G: Nucl. Phys. 7 (1981) 737.
[13] M.A. Caprio, D.J. Rowe, T.A. Welsh, Comput. Phys. Comm. 180 (2009) 1150.
[14] T.A. Welsh (2008) (unpublished).
[15] M.A. Caprio, Phys. Rev. C 72 (2005) 054323.
[16] D.J. Rowe, T.A. Welsh, M.A. Caprio, Phys. Rev. C 79 (2009) 054304.
[17] H. Feshbach, F. Iachello, Phys. Lett. B 45 (1973) 7.
[18] H. Feshbach, F. Iachello, Ann. Phys. (N. Y.) 84 (1974) 211.
[19] J. Janssen, R.V. Jolos, F. Dönau, Nucl. Phys. A 224 (1974) 93.
[20] J. Meyer-ter-Vehn, Phys. Lett. B 84 (1979) 10.
[21] O. Castaños, E. Chacón, A. Frank, M. Moshinsky, J. Math. Phys. 20 (1979) 35.
[22] A.E.I. Dieperink, O. Scholten, F. Iachello, Phys. Rev. Lett. 44 (1980) 1747.
[23] J.P. Elliott, P. Park, J.A. Evans, Phys. Lett. B 171 (1986) 145.
[24] L. Wilets, M. Jean, Phys. Rev. 102 (1956) 788.
[25] D.J. Rowe, G. Thiamova, Nucl. Phys. A 760 (2005) 59.
[26] G. Thiamova, D.J. Rowe, Eur. Phys. J. A 41 (2009) 189.
[27] A. Arima, F. Iachello, Ann. Phys. 123 (1979) 468.
[28] G. Thiamova, Eur. Phys. J. A 45 (2010) 81.
[29] P. Van Isacker, Phys. Rev. Lett. 83 (1999) 4269.
[30] K.Heyde.P. Van Isacker, M. Waroquier, J. Moreau, Phys. Rev. C 29 (1984) 1420.
[31] J.P. Elliott, J.A. Evans, P. Van Isacker, Phys. Rev. Lett. 57 (1986) 1124.
[32] T.D. Cohen, Phys. Rev. C 38 (1988) 1038.
[33] J. Meyer-ter-Vehn, Nucl. Phys. A 249 (1975) 111.
[34] A.S. Davydov, G.F. Filippov, Nucl. Phys. 8 (1958) 237.
[35] A.S. Davydov, A.A. Chaban, Nucl. Phys. 20 (1960) 499.
[36] D.J. Rowe, Rep. Progr. Phys. 48 (1985) 1419.
[37] P.S. Turner, D.J. Rowe, Nucl. Phys. A 756 (2005) 333.
[38] M.A. Caprio, Phys. Rev. C 83 (2011) 064309.
[39] F. Iachello, Phys. Rev. Lett. 91 (2003) 132502.
[40] K. Kumar, Phys. Rev. Lett. 28 (1972) 249.
[41] D. Cline, Annu. Rev. Nucl. Part. Sci. 36 (1986) 683.
[42] J.P. Elliott, P. Van Isacker, Phys. Rev. Lett. 57 (1986) 1124.
[43] R.V. Jolos, P. von Brentano, N. Pietralla, I. Schneider, Nucl. Phys. A 618 (1997) 126.
[44] W. Werner, C. Scholl, P. von Brentano, Phys. Rev. C 71 (2005) 054314.